

*The object of this study is the process of generating cavitation pressure fluctuations behind the throttle device at high-head throttling of liquid. This paper addressed the problem of calculating the amplitude of cavitation pressure fluctuations at high-pressure liquid throttling. It was established that cavitation pressure fluctuations are a consequence of collisions of discrete masses of a transiting liquid jet in the region of pressure recovery. The range of cavitation pressure fluctuations reaches the pressure values at the inlet to the throttle device. The frequency band of cavitation pressure fluctuations is in the range from 1.5 to 20 kHz and higher. At high-head throttling of the liquid, caverns attached to the surface of the throttle channel, moving caverns and small bubbles in the transit flow are formed. Moving caverns compress the transit flow and divide it into separate fluid blocks. In the region of pressure restoration, the moving caverns are slammed shut and discrete fluid blocks collide. This causes high-frequency pressure fluctuations. Special feature of the results is the possibility of estimating the range of cavitation pressure fluctuations depending on the pressure drop on the throttle device. When the back pressure on the throttle device increases, the amplitude of cavitation pressure fluctuations decreases, and the frequency band shifts to the high-frequency region. The results make it possible to calculate the range of cavitation oscillations, to predict the development of cavitation erosion of materials depending on the parameters of throttling of the working fluid. The results of the work are used to design devices for cleaning products from contamination, for determining the volume content of water in aviation fuel, for intensification of technological processes in the chemical and food industries*

*Keywords: cavitation flow, pressure pulsations, pressure drop, discrete jet, high-head throttling*

# DETERMINING THE MECHANISM FOR GENERATING CAVITATION PRESSURE FLUCTUATIONS IN THROTTLE DEVICES AT HIGH-HEAD THROTTLING OF LIQUID

**Taras Tarasenko**  
PhD\*

**Valerii Badakh**  
Corresponding author  
PhD\*

E-mail: bad44@ukr.net

**Mykola Makarenko**  
PhD

Department of Computer Technologies for Design and Graphics\*\*

**Pavel Lukianov**  
PhD\*

**Igor Dubkovetskiy**  
PhD

Department of Processes and Apparatus of Food Production  
National University of Food Technologies  
Volodymyrska str., 68, Kyiv, Ukraine, 01601

\*Department of Hydro-Gas Systems\*\*

\*\*National Aviation University

Liubomyra Huzara ave., 1, Kyiv, Ukraine, 03058

Received date 06.06.2024

Accepted date 12.08.2024

Published date 29.08.2024

**How to Cite:** Tarasenko, T., Badakh, V., Makarenko, M., Lukianov, P., Dubkovetskiy, I. (2024). Determining the mechanism for generating cavitation pressure fluctuations in throttle devices at high-head throttling of liquid. *Eastern-European Journal of Enterprise Technologies*, 4 (7 (130)), 21–31. <https://doi.org/10.15587/1729-4061.2024.309656>

## 1. Introduction

Hydrodynamic cavitation is the formation, growth, and collapse of caverns, which are filled with a mixture of gas and steam of the working fluid [1]. The process of bubble formation occurs when the local flow rate increases so much that the pressure decreases to the pressure of the cavitation threshold (slightly higher than the pressure of saturated vapor at a given temperature). Cavern collapse leads to the appearance of local micro-jets or local shock waves, which mechanically act on the surface in contact with the fluid flow, causing erosion of this surface [2, 3]. Particularly important for cavitation erosion is the explosive asymmetric collapse of the cavern near the wall, which can cause very fast micro-jets up to 400 m/s and shock waves from 6000 to 9000 bar [4].

Calculations of cavitation characteristics of throttle devices require a quantitative assessment of the degree of development of cavitation processes. In an ideal case, the cavitation criterion (Reynolds number, Strouhal number, etc.) for similar geometric and dynamic conditions can be used to estimate the degree of development of the cavitation process regardless of other factors. In reality, the nature and intensity of the cavitation process depends on a large number of factors, the influence of which is complex and not fully studied [5]. The cavitation criterion is a complex function of many variables. The existing criteria are not universal in nature but make it possible to estimate the degree of evolution and dynamics of the process in a first approximation. Their application, taking into account known limitations, does not cause complications in engineering practice [6].

Cavitation outflow of liquid through a throttle device [7] is accompanied by significant pressure fluctuations in the volume behind the throttle device. The amplitude of such pressure fluctuations can reach values close to two supply pressures at the inlet to the throttle device. Therefore, the throttle device can be used as a cavitation generator of pressure fluctuations. The amplitude of these oscillations depends on the pressure drop across the throttle device [8]. Pressure fluctuations in the volume behind the throttle device will initiate a more intense collapse of small bubble caverns [9] with more intense micro-jets and shock waves. These factors will cause more intense mechanical stresses in materials and the growth of cavitation erosion. Therefore, it is necessary to carry out scientific studies into the features of cavitation at high-head throttling of liquid through a throttling device. The results could improve the efficiency of cavitation technologies in the field of cavitation cleaning of surfaces from contamination [10], cavitation drilling, intensification of technological processes in the chemical and food industries, etc.

---

## 2. Literature review and problem statement

---

Cavitation in the hydraulic system is an undesirable phenomenon. It damages the units of the hydraulic system [11], leads to intense pressure fluctuations, to the degradation of the working fluid [12], so cavitation in hydraulic systems should be avoided. In works [11, 12], the mechanism for generating cavitation pressure fluctuations in the liquid volume was not considered, but only from the slamming of small bubbles. The issue of the influence of large-scale factors on pressure fluctuations remains unresolved. In [13], the authors studied pressure fluctuations caused by an unsteady cavitation flow with special emphasis on quasi-periodic cloud cavitation. But the issue of generating pressure fluctuations by detaching a part of the attached cavern in the throttle channel was not considered. The reason for this may be objective difficulties associated with the rapidity of the process by changing the hydrodynamic parameters of the flow.

Papers [14, 15] considered cavitation in throttle devices. Detailed attention is paid to cavitation hydraulics. The critical outflow parameters uniquely determine the values of the hydraulic coefficients for the studied range of Reynolds numbers of the fluid flow. The values of dimensionless hydrodynamic coefficients in the case of cavitation leakage can be calculated from their known values at the cavitation boundary. Due to the fact that the calculation method requires knowledge of the flow coefficients, a large number of spills of throttle devices of various types used in the hydraulic drive were carried out, including confusor-diffuser nozzles, cylindrical chokes, flat and round spools, valves, and other elements [15]. The Rayleigh-Plesset equation for the dynamics of a single bubble was used as a model of pressure fluctuations. But the issues of the influence of vortex structures on the generation of cavitation pressure fluctuations and the influence of the geometry of the throttle device on the parameters of cavitation fluctuations remained unresolved. The reason for this may be certain difficulties associated with the duration of the experiment and errors in the calculation models. In [16], the authors determined the rational geometric parameters of throttle devices with the maximum range of cavitation liquid flow, intended for use in cavitation

devices. But the question of the impact of the pressure drop on the throttle device on the range and frequency of cavitation pressure fluctuations remained unresolved.

The mechanism for the self-excitation of self-oscillations of pressure associated with the pulsation of the dimensions of a settled cavitation cavity in a Venturi tube is proposed in [17]. In the considered mechanism for generating pressure fluctuations, the supply of energy to the oscillating system is determined, according to the author, by the change in pressure losses due to the sudden expansion of the flow behind the cavitation cavern. Pressure losses in the considered mechanism depend on the dimensions of the cavern and the velocity of the liquid in the sections where the cavern is closed. The frequency of cavitation pressure fluctuations is determined by the inertial resistance of the pipeline behind the venturi tube and the compliance of the cavitation zone in the tube. But the author does not explain the mechanism for generating high-frequency pressure fluctuations. The reason for this can be attributed to the difficulties associated with measuring high-frequency pressure fluctuations. A wide range of cavitation pressure pulsations is given in [18]. Thus, the influence of geometric characteristics of the throttle device, throttle parameters on the magnitude of cavitation pressure pulsations has not been fully studied. Other authors provide data [19] that the generation of cavitation pressure fluctuations in the Venturi tube is dominated by vortex structures that have three different states and are stochastic in nature. But they do not take into account the mechanism for the self-oscillations of pressure associated with the pulsation of the dimensions of a settled cavitation cavity.

Paper [20] proposed a model for generating cavitation pressure fluctuations, which is based on a discrete jet model. The model takes into account the effect of the steam-gas mixture, which is released in the cavitation zone, on pressure fluctuations, as well as additional acceleration of the transit liquid jet due to the occurrence of discontinuities in it. The essence of the discrete model is that in the case of high-pressure leakage of liquid through the throttle device (cavitation generator of pressure fluctuations) in the rarefaction zone, the continuous stream is previously divided by steam-gas mobile cavities into separate blocks. Then, in the zone of restoration of integrity, these blocks collide with the flow of retarded liquid, generating pulsations (oscillations) of pressure. Shock waves arising from the cavitation outflow of liquid through a throttle device initiate the collapse of small bubbles [21]. The collapse of bubbles causes a high-frequency component of pressure fluctuations. It is quite difficult to measure the range of pressure fluctuations due to the bursting of the bubble. Therefore, the authors estimated the range of pressure fluctuations according to the nature of damage caused by cavitation erosion of the surface. The reported mechanism of cavitation pressure oscillations is not fully elucidated and requires further research.

For the development of cavitation technologies, designing throttle-type cavitation generators of pressure fluctuations and devising methodology for engineering calculation of their parameters are of great interest. These parameters, with a certain geometric configuration and with a certain pressure drop across them, produce a wide band of cavitation pressure fluctuations. At the same time, different mechanisms of generating pressure fluctuations should be taken into account: the movement of discrete masses of liquid in the throat of the throttle device, pulsations of a collapsed cavern, vortex structures, the collapse of small bubbles nec-

essary for the intensification of the technological process. After all, cavitation pressure fluctuations initiate cavitation erosion of structural materials, liquids, suspensions. Cavitation and cavitation erosion have been studied for more than a century, but until now it has not been definitively established which erosion mechanism dominates. There are two mechanisms for surface destruction due to implosion from bubble collapse. This is the mechanism of generating a shock wave during the collapse of a bubble or cloud of bubbles and the mechanism of a cumulative jet caused by an individual bubble. It is known that high pressure peaks that occur due to the collapse of bubbles cause damage to structural materials. In [22], the results of research on cavitation erosion are given. The authors claim that cavitation erosion is caused mainly by the group collapse of bubbles near the surface of a solid under the action of large-scale hydrodynamic mechanisms. At the same time, pressure pulsations from the group collapse of bubbles cause plastic deformation of the surface. The results of work [23] confirm the results reported in [22] and include data according to which water hammer pressure can cause twice the maximum plastic deformation compared to shock wave deformation, but the impact volume is very small. On the other hand, the shock wave generated by the collapse of the bubble can plasticize 800 times the volume, resulting in a higher rate of surface erosion. However, the authors of [23] did not take into account the large-scale mechanisms of cavitation pressure fluctuations.

In addition to the micro-scale dynamics of micro bubbles, the assessment of cavitation erosion of surfaces requires the analysis of large-scale hydrodynamic mechanisms. Paper [24] describes the development of a cavitation-induced erosion risk assessment tool, which links predictions of multiphase flow modeling with the intensity of material erosion. The evolution of multiphase flow in the channel was modeled using a compressible mixture model, in which the phase change was represented by a homogeneous relaxation model, and the development of turbulent flow was modeled on the basis of a dynamic structure for simulating large eddies. The author estimated the incubation period of cavitation erosion using the stored energy method. Localization of erosion took place in the throttle channel. But the author did not provide data on the course of cavitation erosion outside the throttle channel. The study of the localization of cavitation erosion outside the throttle channel would make it possible to devise an effective technology for cleaning surfaces from contamination, emulsifying mixtures, etc.

Thus, as demonstrated in our review of the literature [13–15, 18, 24], each of the authors cited above investigated one of the mechanisms for cavitation pressure oscillation generation and did not take into account the influence of other mechanisms. Or other mechanisms were weakly manifested. Therefore, the study of cavitation flow, in particular cavitation pressure fluctuations, which are the cause of cavitation erosion, is relevant. The interaction of various mechanisms for generating cavitation pressure fluctuations at high-head liquid throttling has not been experimentally investigated. Dominance of mechanisms for generating cavitation pressure fluctuations under different conditions. All this gives reason to assert that it is expedient to conduct a study on confirming the dominance of the discrete mechanism for generating cavitation pressure fluctuations at high-head liquid throttling. First of all, it is necessary to establish the dependence of pressure drop on the throttle device and the influence of features of the geometry of the throttle

device on the range and frequency of cavitation pressure fluctuations. The research data will provide an opportunity to devise engineering procedures for evaluating cavitation effects in order to develop new cavitation technologies.

---

### 3. The aim and objectives of the study

---

The purpose of our study is to build a mathematical model for estimating the range of cavitation pressure fluctuations at high-head liquid throttling based on experimental research. This will make it possible to design highly efficient cavitation generators of throttle-type pressure fluctuations for the intensification of technological processes that use cavitation technology.

To achieve this goal, the following tasks were solved:

- to investigate the cavitation area using visual studies and measure the distribution of static and dynamic pressure in the cross-sections of a throttle channel;
- to confirm the large-scale mechanism for cavitation pressure oscillation generation behind the throttling device and to build a physical model of the mechanism for cavitation pressure oscillation generation at high-head liquid throttling;
- to evaluate the effectiveness of the throttle cavitation device and investigate the peculiarities of cavitation pressure fluctuations.

---

### 4. The study materials and methods

---

The object of our study is the process of generating cavitation pressure fluctuations in the throttle device at high-head fluid outflow based on the hypothesis of a discrete jet.

The research was carried out on a hydraulic bench (Fig. 1), which is an installation that makes it possible to perform experiments to determine dynamic phenomena in throttle devices of various types. Also, the installation allows for visual observations of cavitation liquid outflow, as well as makes it possible to determine parameters of cavitation liquid outflow.

The main assumptions in this work are cavitation is steam-gas, flow parameters are average, pipeline walls are rigid, liquid is compressible.

The basis of our research was a comprehensive method, which involves the joint use of physical and mathematical modeling of cavitation processes in throttle devices with further experimental confirmation of the adequacy of results.

A measuring tank with a volume of 10 dm<sup>3</sup> with a calibration accuracy of  $\pm 5$  cm<sup>3</sup> was used to measure the flow rate. The time of filling the measuring tank was determined by an arrow stopwatch with a division value of 0.05 s. Taking into account the phenomenon of lubrication when emptying the measuring tank, measurements were performed at three-minute intervals. For the range of volumes from 1000 to 3000 cm<sup>3</sup>, the relative measurement error was from  $\pm 1.2$  % to  $\pm 0.6$  %.

Control over the density of the working fluid was executed with a hydrometer with an accuracy of 0.05 %. The viscosity of the liquid was measured by a VK type viscometer according to the standard method. Experimental studies on the hydraulic bench were carried out under the following conditions: atmospheric pressure,  $760 \pm 20$  mm Hg; air temperature, from 10 to 25 °C. The relative humidity of the air was  $65 \pm 15$  %.

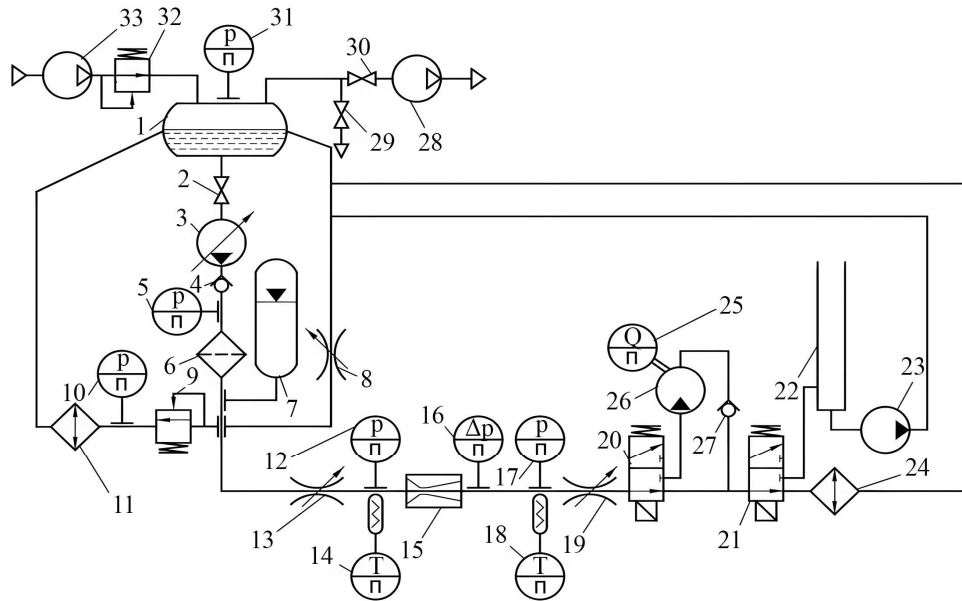


Fig. 1. Basic hydraulic scheme of the experimental bench for the study of cavitation effects: 1 – hydraulic tank; 2, 29, 30 – shut-off valves; 3 – volumetric pump; 4, 27 – check valves; 5, 10, 12, 17, 31 – manometers; 6 – filter; 7 – hydraulic accumulator; 8, 13, 19 – throttle valves; 9 – safety valve; 11, 24 – heat exchangers; 14, 18 – thermometers; 15 – cavitation generator; 16 – pressure pulsation sensor; 20, 21 – electromagnetic taps; 22 – measuring tank; 23 – centrifugal pump, 25 – flow meter sensor, 26 – flow meter, 28 – vacuum pump, 32 – reducer; 33 – compressor

Visual studies of cavitation jets were performed on transparent models of cavitation generators of pressure fluctuations with pulsed illumination of the liquid flow “into the light”. The duration of illumination was two orders of magnitude shorter than the duration of the cavitation cavity (Fig. 2).

The liquid flow was photographed in the reflected light of two lamps, which corresponds to the visual perception of the flow. The scheme of photographing “into the light” is shown in Fig. 2. The cavitation flow was photographed by a high-speed camera SFR-2M.Δp.

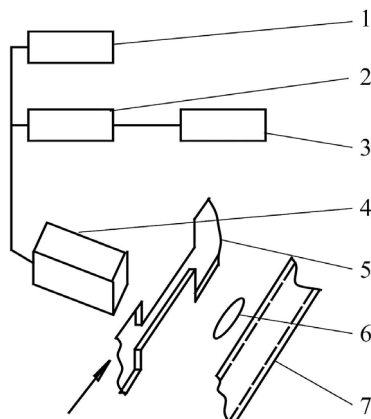


Fig. 2. Photographing schematics: 1 – pulse discharge device; 2 – a battery of capacitors; 3 – direct current source; 4 – illuminator; 5 – throttle channel; 6 – receiving optical system; 7 – photographic film

possible to establish the relationship between the hydrodynamic parameters of the flow and the evolution of cavitation. The structure of the cavitation flow is observed on transparent models of throttle devices using photography.

The resulting fluid flow patterns are compared with the hydraulic characteristics of throttle devices. Visual observations of the flow of AMG-10 liquid in a choke with a rectangular channel make it possible to monitor changes in the structure of the cavitation flow [9]. In the range of pressure drops  $0 < \Delta p < 0.31$  ( $p_{in}^{abs} = 1.06$  MPa,  $Re = 2,620$ ), the flow along the entire channel has a transparent appearance. Stagnant zones in the flow behind the inlet edges become visible at  $Re > 2,620$ . The first discontinuities in the flow occur at a pressure drop  $\Delta p = 0.58$  ( $Re = 4,855$ ). The flow pattern corresponding to the beginning of cavitation is shown in Fig. 3. Shooting was done in reflected light with an exposure  $f_e = 2 \cdot 10^{-3}$  s.

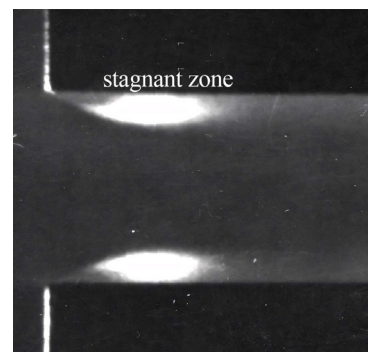


Fig. 3. Formation of stagnant zones in the flow of liquid;  $\Delta p = 0.58$ ; magnification  $\times 23$

## 5. Results of investigating the mechanism for cavitation pressure oscillation generation

### 5. 1. Visualization of the cavitation flow

The study of the structure of the cavitation flow is important for explaining the nature of cavitation and makes it

The rearrangement in the flow structure, which manifests itself in the appearance of gas bubbles on the walls of the channel behind the inlet edges, occurs at  $\Delta p = 0.64$  (Fig. 4). Discontinuity breaks occur only in the boundary layer of the

flow separation zone from the sharp edges of the throttle surfaces with a rectangular channel. Cavitation does not extend to the core of the flow.

Bubble caverns move within the stagnation region, undergoing phases of growth and destruction. The greater the pressure drop across the throttle, the larger the caverns (Fig. 4, *b, c*). Caverns that reach the place of re-attachment of the jet to the walls of the throttle are destroyed. The destruction of caverns lasts about 20 μs (Fig. 4, *b*; frames 2–6). Dissolution of the gas phase and condensation of steam is completed inside the throttle channel.

The peculiarity of liquid flow with stabilization of its consumption ( $\Delta\bar{p} \geq 0.70$ ; developed cavitation) is as follows. Caverns attached to the wall of the channel are formed in the stagnant areas of the flow, and in the compressed jet, non-spherical moving caverns appear.

Moving caverns can be commensurate with the size of the channel (Fig. 5). On the cinematographs, the attached caverns are marked with the letter A; moving caverns – by the letter B. The period of occurrence of moving caverns ranges from  $10^{-4}$  to  $10^{-5}$  s (the frequency of film registration is 325,000 frames/s). In the growth phase, simultaneous stretching of the cavern along the flow and increase in its cross-section is observed.

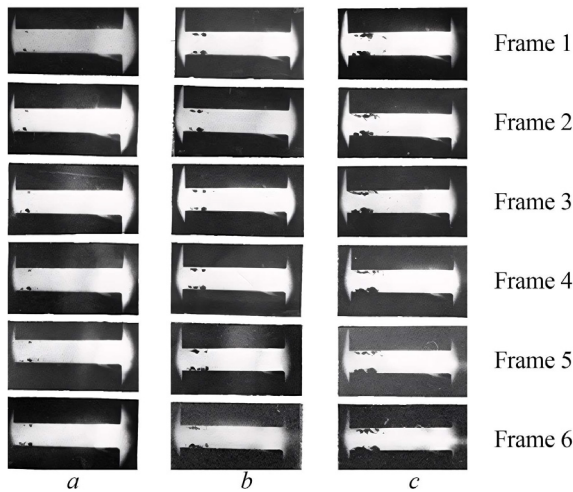


Fig. 4. Caverns in the stagnant flow region of a rectangular throttle at the initial stage of cavitation evolution: *a* –  $\Delta\bar{p}=0.58$ ; *b* –  $\Delta\bar{p}=0.64$ ; *c* –  $\Delta\bar{p}=0.66$

In the growth phase, simultaneous stretching of the cavern along the flow and increase in its transverse size is observed. According to Fig. 5, *b*, the growth rate of the length of the cavern in the initial phase, in the direction of the flow, exceeds the liquid flow rate by approximately 1.5 times. The maximum length of such a cavern can reach the length of the cavitation zone, and the flow break occurs along the entire live section. As the aft part of the cavern approaches the limit zone of cavitation, the growth rate of its length decreases. After equalizing the growth rates of the cavern and the current, the cavern is swept away by the current.

The shape of flow discontinuities is usually not repeated. The formation of cavities from cavitation nuclei moving in the center of the jet is blocked by the development of peripheral gaps. The development of both single and interacting caverns is possible. The moving caverns, in the process of growth, divide the transit stream into separate volumes of liquid.

Therefore, the physical model of the cavitation flow cannot be described by the homogeneous gas-liquid flow model, which assumes a uniform distribution of the liquid and gaseous phases in the flow.

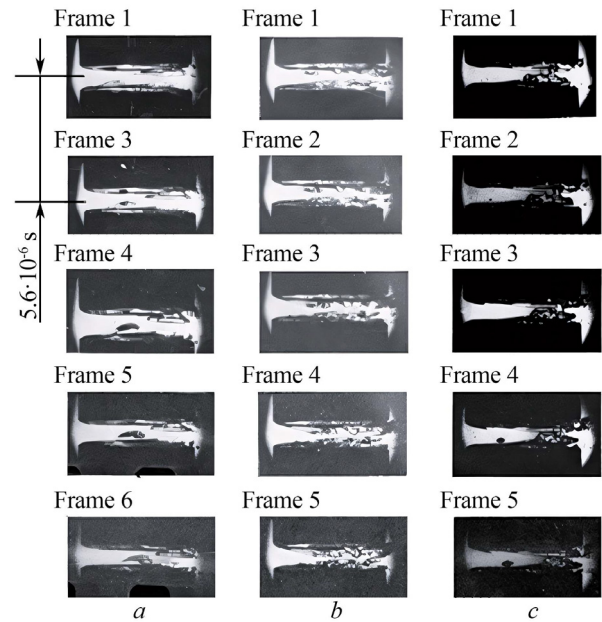


Fig. 5. Caverns in the liquid flow with developed cavitation: *a* –  $\Delta\bar{p}=0.74$ ; *b* –  $\Delta\bar{p}=0.78$  *c* –  $\Delta\bar{p}=0.81$

Moving caverns with advanced cavitation collapse according to different patterns than caverns at the stage of initial cavitation. At the initial cavitation, the bubbles are destroyed by closing. With advanced cavitation, the cavern breaks up into smaller bubbles as its stern reaches beyond the cavitation zone. Smaller caverns are closed, and the flow behind the cavitation zone is enriched with gas.

With a significant decrease in back pressure, a super cavitation regime may occur, under which the vapor-gas attached cavity goes beyond the limits of the throttle channel.

Repeated breaks in the integrity of the liquid under the mode of advanced cavitation can occur behind the throttle channel (Fig. 6). Caverns are formed in the centers of converging vortices when the back pressure behind the throttle is a few percent of the supply pressure.

To find out the nature of cavitation in hydraulic drive devices, it is necessary to establish the relationship between the hydrodynamic parameters of the flow and the observed breaks in the continuity of the working medium.

Fig. 7 shows the diagrams of static pressure distribution in the cross sections of the throttle rectangular channel with initial ( $\Delta\bar{p}=0.58$ ) and advanced cavitation ( $\Delta\bar{p}=0.81$ ). The pressure was measured by scanning the receiving holes of the channel wall gauge. The pressure receiver was moved by a micrometer screw perpendicular to the liquid flow. On the basis of the measurements, the diagrams of pressure distribution in the control sections were constructed.

Based on the results of the considered diagrams, regardless of the liquid flow regime, the following characteristic sections of the flow can be distinguished: the inlet, the compressed section of the jet, pressure recovery, and stagnant areas.

Comparing the diagrams (Fig. 7) with the photographic images of the flow (Fig. 4, 5), the following features of the flow should be noted. During the initial cavitation, the places of

genesis and development of the moving caverns coincide with the position of the maximum pressure gradient at the boundary of the compressed jet and the stagnant zone. This confirms the vortex nature of the occurrence of discontinuities when the pressure in the center of the vortex drops to the threshold.

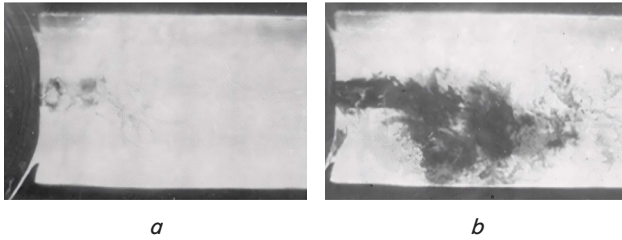


Fig. 6. Caverns in the drain line behind the throttle: *a* –  $\Delta\bar{p}=0.78$ ; *b* –  $\Delta\bar{p}=0.88$

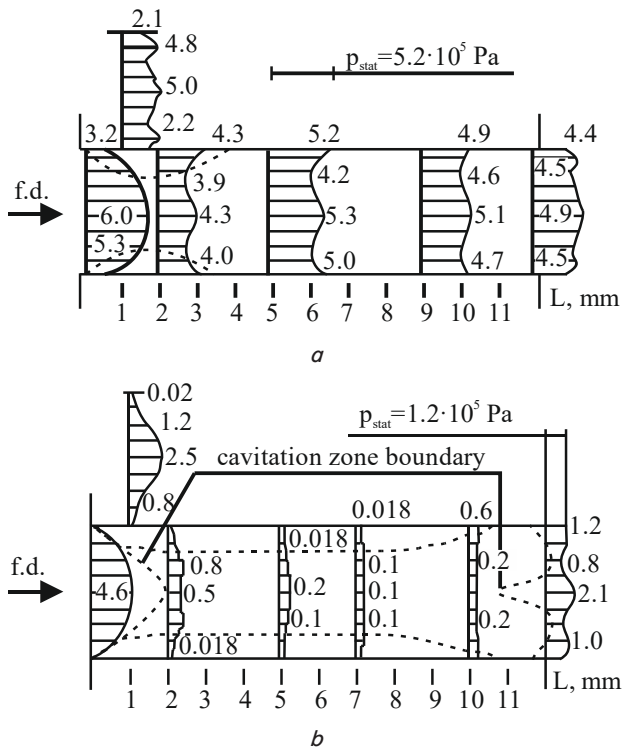


Fig. 7. Diagrams of distribution of static pressure in the intersections of a choke with a rectangular channel: *a* –  $\Delta\bar{p}=0.58$ ; *b* –  $\Delta\bar{p}=0.81$

With developed cavitation, the liquid flow rate, and accordingly the flow rate in the inlet section, stabilizes and does not depend on the back pressure in the drain line behind the throttle. Stabilization of the liquid flow rate is associated with the establishment of a constant pressure drop from the inlet to the compressed cross-section of the jet. The minimum pressure recorded in the connected caverns (cavitation threshold pressure) was 1.8 kPa (14 mm Hg). Some change in pressure along the height of the channel is associated with the retarding effect of the channel walls during jet inversion.

The rarefaction zone on the diagrams coincides with the visual picture of the location of the quasi-resistant connected caverns. The complex configuration of the boundary of the cavitation zone in the throttle channel is determined by the dynamic interaction of the compressed jet with the flow outside the region of reduced pressure.

The characteristic features of the pressure distribution in the cylindrical channel are that in the inlet part of the flow, the static pressure drops sharply due to the acceleration of the narrowing flow (Fig. 8). Compared to axial jets (curves 6–10), the pressure drops more intensively in the wall region (curves 1–5). Under the regimes of initial cavitation  $0.56 \leq \Delta\bar{p} \leq 0.59$ , the annular stagnation region of the flow behind the inlet edge is evacuated (curve 2). As cavitation intensifies, the vacuum zone spreads along the length of the throttle channel. The static pressure in the compressed section of the jet also falls as the pressure drop across the throttle channel increases and reaches a minimum value (cavitation threshold pressure) when  $\Delta\bar{p} = \Delta\bar{p}_{crit}$  (curves 7, 8). The cross-section of the flow, in which the threshold pressure is fixed, is removed from the inlet edge by a distance that is approximately equal to half the diameter of the throttle opening *d*. Subcritical flow regimes at  $\Delta\bar{p} = \Delta\bar{p}_{crit}$  are characterized by the spread of the cavitation threshold pressure zone in the flow direction, and upon reaching the drop  $\Delta\bar{p} = 0.80$ , the entire volume of liquid in the channel is subject to vacuuming (curves 4, 5, 9, 10).

The dynamic pressure was recorded along the axis of the cylindrical channel in three cross-sections of the flow: inlet, compressed, and outlet. Flow regimes without cavitation and initial cavitation are accompanied by an increase in dynamic pressure in all flow control cross-sections under the condition of an increase in the pressure drop across the throttle (Fig. 9). At subcritical flow regimes due to the establishment of a constant pressure difference between the inlet and compressed sections, the fluid flow rate in this gap stabilizes and does not depend on back pressure (curves 1, 3). The dynamic pressure behind the nozzle, despite the stabilization of the liquid mass flow rate, continues to increase as the pressure drop increases (curve 2). Additional acceleration of the flow is associated with a violation of the continuity of the liquid.

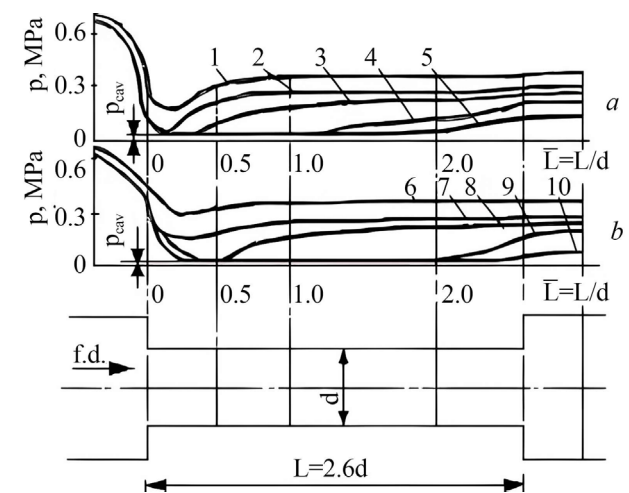


Fig. 8. Distribution of static pressure along the flow length in a cylindrical throttle: *a* – in the near-wall region; *b* – along the axis of the channel; 1, 6 –  $\Delta\bar{p}=0.47$ ; 2, 7 –  $\Delta\bar{p}=0.56$ ; 3, 8 –  $\Delta\bar{p}=0.59$ ; 4, 9 –  $\Delta\bar{p}=0.65$ ; 5, 10 –  $\Delta\bar{p}=0.84$

In a choke with a rectangular channel, the flow velocity was measured in a continuous flow with a single-component laser Doppler meter, and in the zone of gaps – by the results of decoding cinemograms.

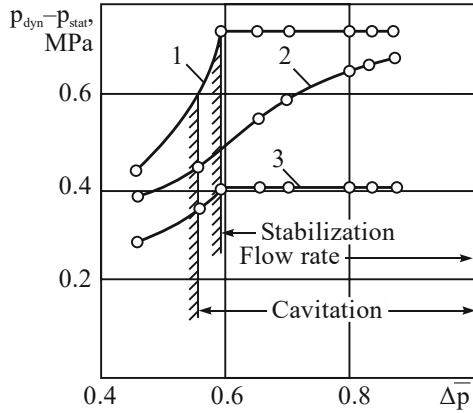


Fig. 9. Dependence of the difference between the dynamic and static flow pressure on the pressure drop across the cylindrical throttle: 1 – compressed cross-section; 2 – initial cross-section; 3 – inlet cross-section

It was found that in the cavitation zone at subcritical flow regimes, the speed of the discrete jet at the time of the development of the moving caverns is approximately 1.5 times higher than the speed of the continuous flow. During the collapse of caverns on the border of the cavitation zone, the flow rate takes on a value determined by the pressure difference between the inlet and compressed sections of the jet. Since the caverns are formed discretely, the acceleration and deceleration of the flow in the cavitation zone has a pulse character. The pulsation of the speed depends on the size of the caverns, and the frequency is determined by the period of their occurrence.

The ratio between the velocities of liquid flow in the cavitation zone and beyond it is approximately determined using Euler's theorem on the change in the amount of movement for the masses of liquid entering the cavitation zone and flowing out of it. The calculation dependence takes the form:

$$V^* = V_{steady} \left( \frac{1}{\varepsilon} + \frac{1}{\mu_{noz}} \sqrt{\frac{\Delta\bar{p} - \Delta\bar{p}_{crit}}{\Delta\bar{p}_{crit}}} \right), \quad (1)$$

where  $V^*$  is the average speed of movement of liquid volumes in the cavitation zone;  $V_{steady}$  – average velocity of liquid flow in the cavitation zone;  $\varepsilon$  – jet compression ratio;  $\mu_{noz}$  – throttle flow coefficient, calculated from the pressure drop  $\Delta\bar{p} = p_{in} - p_{out}$ ;  $\Delta\bar{p}$  – pressure drop on the throttle device;  $\Delta\bar{p}_{crit}$  – critical pressure drop on the throttle device.

### 5. 2. Model of the generation of cavitation pressure fluctuations in the volume behind the throttle device

Based on our research, a physical model of cavitation pressure fluctuations was built. This model is based on the use of the Bord theorem. The use of Bord's theorem for flow breaks is justified by the fact that it is based on the theorem of impulses, the use of which is also appropriate in the case of the movement of discrete liquid masses. We assume that the boundaries of the cavitation zone have the form of flat cross sections. Sections for writing equations are marked 1–1 and 2–2, respectively (Fig. 10). The integrity of the fluid up to cross-section 1–1 is not yet broken, and it is restored again in cross-section 2–2. At all points of the cavitation zone, the pressure is equal to the pressure of the cavitation threshold  $p_{cav}$ .

Liquid flow velocities at the boundaries of the cavitation zone  $V_{comp}$  and  $V_{steady}$  are considered as average flow

rates and are determined from the flow equation. Under the critical cavitation regimes, the average flow rate of discrete volumes in the cavitation zone increases from  $V_{comp}$  to  $V^*$  and in cross-section 2–2 the flow slows down from  $V^*$  to  $V_{steady}$ . Experimentally, the instantaneous values of the average speed are determined by deciphering the filmograms.

As the pressure drop increases, the length of the cavitation zone and the degree of flow acceleration increase. Thus, the pressure difference  $p_{out\_crit} - p_{crit}$  characterizes the degree of two-phase flow and the degree of acceleration of the discrete jet.

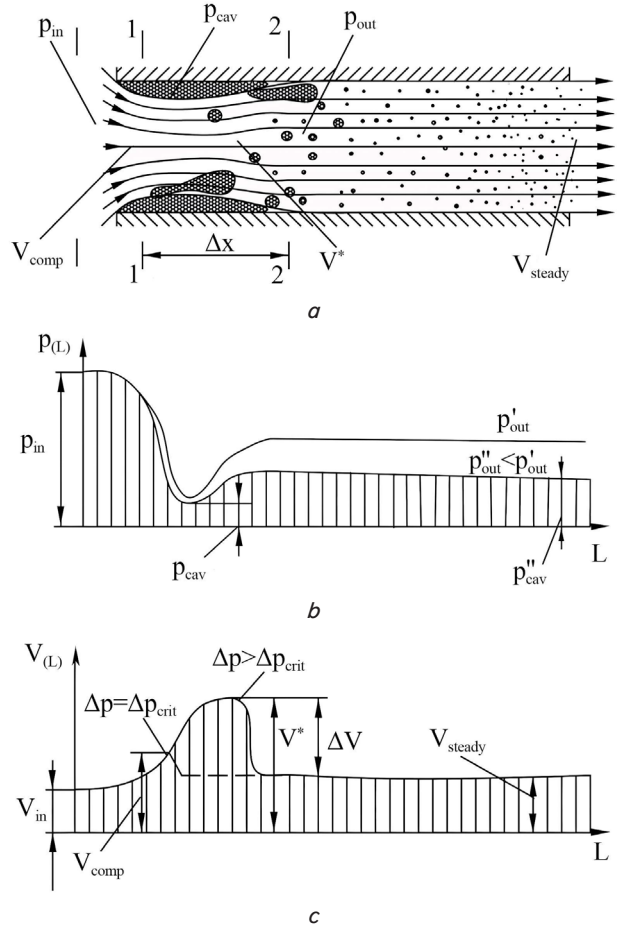


Fig. 10. Cavitation outflow of liquid through a cylindrical throttle: a – distortion of flow lines and generation of caverns; b – pressure change in the flow; c – change in flow rate

Equating the amount of fluid movement in the compartment between cross-sections 1–1 and 2–2 to the momentum of the main vector of surface forces, we obtain:

$$\delta p_i = \rho a(\bar{p}) V_{steady} \left( \frac{V^*}{V_{steady}} \Delta\bar{\omega} - 1 \right), \quad (2)$$

where  $\rho$  – liquid density;  $\Delta\bar{\omega}$  – the degree of discreteness of the jet;  $\delta p_i$  is the range of cavitation pressure fluctuations;  $a(\bar{p})$  is the propagation speed of an elastic wave in a liquid in the cavitation region:

$$a(\bar{p}) = \frac{a_{liq}}{\sqrt{1 + \frac{\bar{Q}_{st.g.} \rho a_{liq}^2}{kp}}}, \quad (3)$$

where  $a_{liq}$  is the propagation speed of an elastic wave in a degassed liquid;  $\rho$  – liquid density;  $k$  is the adiabatic index;  $p$  is the pressure at the inlet to the throttle device;  $\bar{Q}_{st.g.}$  – volumetric content of the steam-gas phase, reduced to atmospheric conditions:

$$\bar{Q}_{st.g.} = \frac{Q_{air}}{Q_{liq}} = \left( \frac{p_{cav} - p_{sat.st.}}{p_{atm}} \right) \left( 1 - \frac{p_{sat.st.}}{p_{cav}} \right) \frac{\varepsilon}{\mu} \sqrt{\frac{\Delta\bar{p} - \Delta\bar{p}_{crit}}{\Delta\bar{p}_{crit}}}, \quad (4)$$

where  $Q_{air}$  – volumetric flow rate of the steam-gas mixture;  $Q_{liq}$  – liquid flow rate;  $p_{cav}$  – pressure in the cavitation zone;  $p_{sat.st.}$  – partial pressure of saturated liquid vapors at a given temperature;  $p_{atm}$  – atmospheric pressure;  $\varepsilon$  – jet compression coefficient;  $\mu$  – flow coefficient of the throttle device;  $\Delta\bar{p}$  – pressure drop on the throttle device;  $\Delta\bar{p}_{crit}$  – critical pressure drop.

For a cylindrical channel  $\Delta\bar{p}_{crit} = 0.59$ ,  $\mu = 0.82$ ,  $\varepsilon = 0.64$ . Saturated vapor pressure for AMG-10 is 0.4 kPa, atmospheric pressure is 100 kPa.

Acceleration of the jet creates conditions for the generation of powerful shock pulses of pressure in the flow behind the cavitation zone. The maximum value of the acceleration speed of the cavitation jet for  $p_{in} = 20$  MPa at  $\Delta\bar{p} = 0.99$  is  $V^* = 238$  m/s. Under such conditions, with a sudden expansion, powerful pressure pulsations are generated with a certain periodicity, which initiate the slamming of small bubbles. Damping of pressure pulsations occurs due to aeration of the flow as it accelerates. The air content increases as the pressure drop increases. The speed of sound wave propagation can be significantly reduced due to aeration.

Our model of the discrete cavitation flow, which occurs under cavitation flow regimes in throttles, makes it possible to explain a wide (from 40 Hz to 200 kHz) spectrum of cavitation pressure fluctuations.

### 5.3. Evaluating the effectiveness of throttle devices and research into cavitation pressure fluctuations

The effectiveness of these throttle devices as cavitation generators of pressure fluctuations can be judged by their energy flow-drop characteristics (Fig. 11)  $(\bar{Q})^2 = f(\bar{p}, \Delta\bar{p})$ , where  $(\bar{Q})^2 = (Q/Q_{calc})^2$  is the square of the dimensionless flow rate of the liquid passing through the throttle device;  $\Delta\bar{p}$  is the relative pressure drop on the throttle device;  $Q$  is the current flow rate value;  $Q_{calc}$  is the calculated (maximum) value of the flow rate.

The energy supplied to the flow with growth  $\Delta\bar{p}$  above the critical value is spent on the formation of cavitation discontinuities. A further increase in the drop over  $\Delta\bar{p}_{crit}$  leads to an increase in the length of the cavitation torch at a constant flow of liquid. Automodelity of the obtained characteristics according to the Reynolds number occurs from the moment of reaching  $Re = 8000$ .

The energy characteristics of generators can be calculated based on the values of flow coefficients when flowing out without cavitation  $\mu_I$  and with cavitation  $\mu_{II}$ . The energy supplied to the flow during cavitation outflow of liquid is:

$$N_{sup} = p_{in} Q_{steady}, \quad (5)$$

where  $Q_{steady}$  is the stabilized flow during cavitation liquid outflow.

Taking into account the fact that during cavitation the power of the spent flow is:

$$N_{cav} = p_{in} (1 - \Delta\bar{p}_{crit}) Q_{steady}, \quad (6)$$

and at zero back pressure, all the energy is spent, part of the cavitation energy is equal to:

$$\frac{N_{cav}}{N_{sup}} = \frac{p_{in} (1 - \Delta\bar{p}_{crit}) Q_{steady}}{p_{in} Q_{steady}} = 1 - \Delta\bar{p}_{crit}. \quad (7)$$

Experimental studies of cavitation pressure fluctuations were carried out at supply pressure values of 8 and 10 MPa. Cavitation pressure fluctuations are shown on channel 2, channel 1 captures pump pulsations (Fig. 12). Cavitation pressure fluctuations, in contrast to pump pulsations, have an inharmonic character, although they can be distinguished as a carrier pump harmonic. Due to the inharmonicity of the oscillations, the range of cavitation pressure oscillations is estimated by the “double amplitude”, which means the value  $\delta p_i = p_{max} - p_{min}$ . The plunger frequency of the pump is 442 Hz.

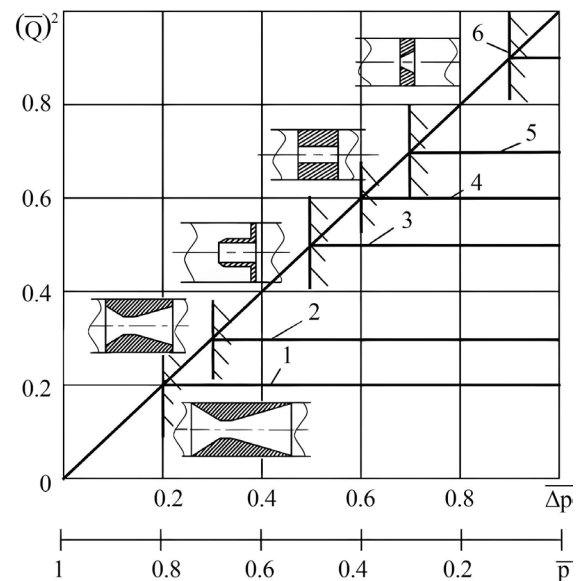


Fig. 11. Flow rate and drop characteristics  $(\bar{Q})^2 = f(\bar{p}, \Delta\bar{p})$  of throttle devices (working fluid AMG-10): 1 – nozzle of the confusor-diffuser type; 2 – nozzle of the confusor-diffuser type, shortened; 3 – Bord nozzle; 4 – cylindrical nozzle; 5 – nozzle with a rectangular channel; 6 – diaphragm

The maximum range of the pulsating pressure is 10 MPa at the supply pressure  $p_{in} = 10$  MPa. This maximum corresponds to the relative pressure drop  $\Delta\bar{p} = 0.85 - 0.95$ . The maximum of the “double amplitude” shock pressure pulsations for the confusor-diffuser nozzle under the regime  $\Delta\bar{p} = 0.95$  occurs at frequencies of 2–7 kHz (Fig. 13).

There is a tendency that when the back pressure at the outlet of the throttle nozzle increases, the spectrum of cavitation pressure fluctuations shifts to the high-frequency region.

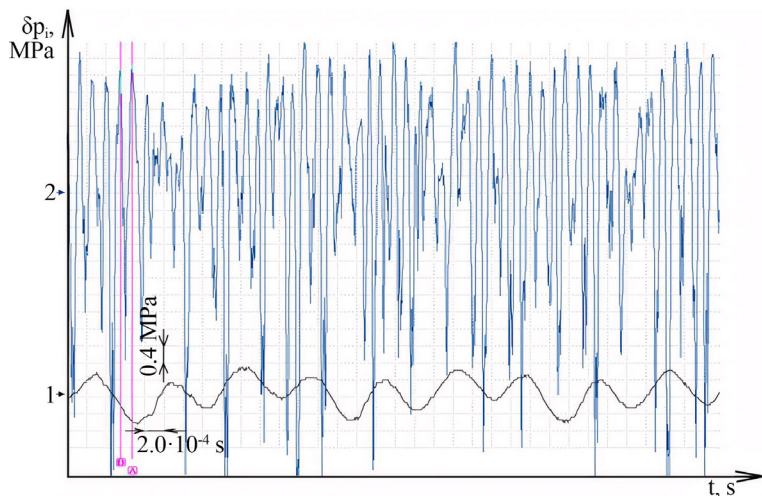


Fig. 12. Cavitation pressure fluctuations behind the confusor-diffuser nozzle ( $\Delta\bar{p}=0.95$ ;  $p_{in}=10$  MPa;  $\delta p_i=10$  MPa): channel 1 – pump pressure pulsations; channel 2 – pressure pulsations behind the confusor-diffuser nozzle

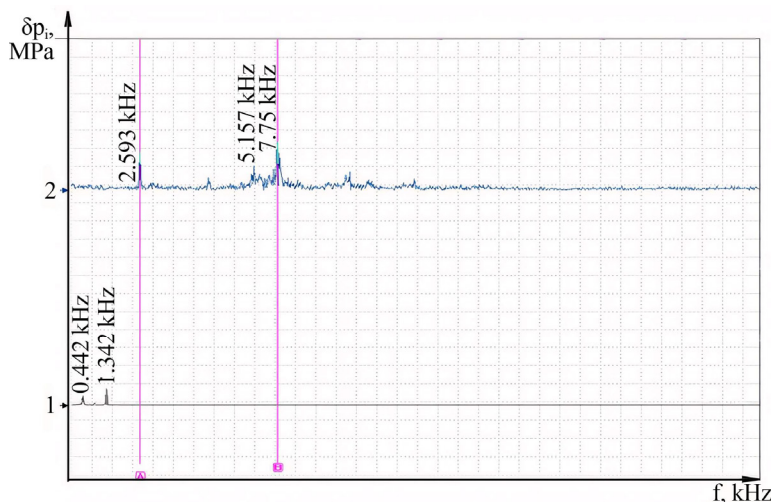


Fig. 13. Spectral characteristics of cavitation pressure fluctuations behind the confusor-diffuser nozzle ( $\Delta\bar{p}=0.95$ ;  $p_{in}=10$  MPa): channel 1 – spectrum of pumping pressure pulsations; channel 2 – spectrum of cavitation pressure pulsations

### 6. Discussion of results of investigating the mechanism of cavitation pressure oscillation generation at high-head liquid throttling

During the study of the cavitation region in the throttle device at high-head throttling of the liquid, a number of features of cavitation flow were established. Caverns connected to the wall of the throttle channel and caverns moving in the transit flow are formed in the throttle channel (Fig. 4, 5). Caverns moving in the transit flow divide the liquid stream into separate blocks. Also, the formation of small bubbles in the transit flow is observed. In contrast to paper [9], in which the cavitation region in the throttle channel was considered as a cloud of small bubbles, moving caverns are considered in our study. With developed cavitation, moving caverns additionally compress the liquid flow and divide it into parts. The presence of attached caverns and caverns that move is confirmed, in addition to visual studies, by

measuring static and dynamic pressures in the throttle channel (Fig. 8, 9). Based on the previous facts, it was found that the flow rate of the liquid phase in the cavitation zone changes impulsively. In the phase of growth of the cavern, the moving flow accelerates, at the moment of its destruction, the flow slows down (Fig. 10). This feature is the reason for the generation of high-frequency pressure fluctuations behind the throttle device, the frequency of which coincides with the frequency of the collapse of moving caverns (Fig. 4, 5). The amplitude of these pressure fluctuations is proportional to the pressure at the inlet to the throttle device (Fig. 12). The specified feature of the cavitation area made it possible to propose a physical model of the generation of cavitation pressure fluctuations in the volume behind the throttle device. The model is based on the division of the transit jet into separate blocks followed by impulse braking of the blocks in the region of restored pressure. The momentum theorem was used to describe this process, which describes the process very well in the case of discrete liquid masses. Formula (2) correlates well with experimental data (Fig. 12). It has been experimentally confirmed that cavitation pressure fluctuations generated by throttle devices are the result of several processes occurring at the macro- and micro-levels. The low-frequency component of cavitation pressure fluctuations (400...800 Hz) is a consequence of modulation of the plunger frequency of the pump with the frequency of descent of discrete liquid masses. The high-frequency component of the spectrum (1...10 kHz and more) of cavitation pressure fluctuations is formed in the form of an ensemble of various processes that occur simultaneously. The main factor of cavitation pressure fluctuations is the collision of discrete masses of liquid with the inhibited flow of liquid (the so-called “projectile” movement of liquid). The next factor in the generation of cavitation pressure fluctuations is the collapse of vortex structures on the throttle nozzle section. The collision of discrete liquid masses and the collapse of vortex

structures initiate the collapse of small bubbles. The given mechanisms of cavitation pressure oscillation generation make it possible to explain the intensive flow of cavitation erosion at high-head liquid throttling. On the basis of the analysis of the flow and differential characteristics of throttle devices of various types, it was established that as generators of cavitation pressure fluctuations, it is advisable to use nozzles of the confusor-diffuser type and cylindrical Venturi nozzles [25] with confusor angles greater than 45°. In our studies, measurements of cavitation pressure fluctuations in the volume at the cut of the throttle device were performed. The potential effect of the studies is to use the energy of the fluid flow to generate pressure fluctuations, without the use of additional equipment.

A limitation of our research is that the given mechanism of impulse braking of the jet dominates only for the condition of high-head throttling of the liquid. The range of cavitation pressure fluctuations calculated by formula (2) has an

averaged value, and the flow parameters in formula (2) are taken as average. The range of pressure drop on the throttle device corresponds to the mode of advanced cavitation and is adequate and the results of the study can be reproduced, leading to the claimed effects.

A drawback of this study is that the measurements of cavitation pressure fluctuations were performed in the volume behind the throttle device. Therefore, pressure pulsation measurements from the collapse of an individual bubble were not performed. This can be estimated by the nature of the cavitation destruction of the test surface. This shortcoming can be eliminated in the future by improving the technology and equipment for measuring rapidly changing pressure.

The development of this study involves improving the model of cavitation pressure oscillation generation, taking into account its stochastic nature and various mechanisms for pressure oscillation generation. On this path, one may encounter difficulties of a mathematical nature (description of the mechanisms of generation of pressure fluctuations) and of an experimental nature (measurement of pressure pulsations during the collapse of a small bubble).

---

## 7. Conclusions

---

1. On the basis of filmograms and pressure measurements in the control cross sections of the throttle channel, the cavitation region was investigated. Two characteristic forms of liquid flow interruption in the throttle device during cavitation operation were established: moving caverns and connected caverns. Moving caverns additionally compress the flow and break it into parts.

2. The large-scale mechanism for cavitation pressure oscillation generation was confirmed. A physical model of the large-scale mechanism for generating cavitation pressure fluctuations in the volume behind the throttle device is proposed. This model predicts a sudden change in the rate of transit fluid flow during the growth and collapse of migrating caverns. At the same time, discrete masses of liquid collide with the inhibited liquid flow, which is the cause of high-frequency pressure fluctuations. A formula for

determining the range of cavitation pressure fluctuations is proposed, which makes it possible to link the operating mode of the throttle device with the range of cavitation pressure fluctuations.

3. The effectiveness of throttle cavitation devices was evaluated according to the experimentally obtained flow-drop characteristics and a rational configuration of the throttle device for converting the energy of the liquid flow into cavitation was established. Peculiarities of cavitation pressure fluctuations were studied. The range of cavitation pressure fluctuations at high-head liquid throttling depends on the pressure drop across the throttling device. With the pressure drop  $\Delta\bar{p}=0.95$  at the supply pressure  $p_{in}=10$  MPa, the range of cavitation pressure fluctuations is  $\delta p_i=10$  MPa. At a pressure drop  $\Delta\bar{p}=0.60$  (the limit of the cavitation regime) at a supply pressure of  $p_{in}=10$  MPa, the range of cavitation pressure fluctuations is  $\delta p_i=4$  MPa.

---

## Conflicts of interest

---

The authors declare that they have no conflicts of interest in relation to the current study, including financial, personal, authorship, or any other, that could affect the study, as well as the results reported in this paper.

---

## Funding

---

The study was conducted without financial support.

---

## Data availability

---

All data are available, either in numerical or graphical form, in the main text of the manuscript.

---

## Use of artificial intelligence

---

The authors confirm that they did not use artificial intelligence technologies when creating the current work.

---

## References

1. Glazkov, M., Lanetskiy, V., Makarenko, N., Chelyukanov, I. (1987). Kavitatsiya v zhidkostnyh sistemah vozdushnyh sudov. Kyiv: KIIGA, 64.
2. Zheng, X., Wang, X., Lu, X., Zhang, Y., Zhang, Y., Yu, J. (2023). An Experimental Study of Cavitation Bubble Dynamics near a Complex Wall with a Continuous Triangular Arrangement. *Symmetry*, 15 (3), 693. <https://doi.org/10.3390/sym15030693>
3. Ohl, C., Linbau, O., Lauterborn, W., Philipp, A. (1998). Details of asymmetric bubble collapse. *Third international Symposium on Cavitation*. Band 1. Grenoble, 39–44.
4. Osterland, S., Müller, L., Weber, J. (2021). Influence of Air Dissolved in Hydraulic Oil on Cavitation Erosion. *International Journal of Fluid Power*, 22 (3), 373–392. <https://doi.org/10.13052/ijfp1439-9776.2234>
5. Glazkov, M., Tarasenko, T. (2003). Vliyanie rezhimov drosselirovaniya na lokalizatsiyu i intensivnost' erozii gidroapparatury v potoke zhidkosti. *Promyslova hidravlika i pnevmatyka*, 2, 43–46.
6. Knepp, R., Deyli, L., Hemmit, F. (1974). Kavitatsiya. Moscow: Mir, 679.
7. Tarasenko, T., Badakh, V. (2017). Cavitation Liquid Leakage through Throttle Device. *Mechanics and Advanced Technologies*, 3 (81), 82–91. <https://doi.org/10.20535/2521-1943.2017.81.117480>
8. Hlazkov, M., Lanetskiy, V., Tarasenko, T. (2007). Matematychna model rozmakhu kavitatsiynykh pulsatsiy tysku. *Materialy IX mizhnarodnoi naukovy-tekhnichnoi konferentsiyi «Avia - 2007»*. Vol. 2. Kyiv: NAU, 60–62.
9. Soyama, H., Hoshino, J. (2016). Enhancing the aggressive intensity of hydrodynamic cavitation through a Venturi tube by increasing the pressure in the region where the bubbles collapse. *AIP Advances*, 6 (4). <https://doi.org/10.1063/1.4947572>

10. Tarasenko, T., Badach, V., Puzik, O. (2013). Functional units based on cavitation effects for hydraulic systems of vehicles. *Science – Future of Lithuania: 16th Conference for Junior Researchers*. Vilnius, 50–54.
11. Xu, X., Fang, L., Li, A., Wang, Z., Li, S. (2021). Numerical Analysis of the energy loss mechanism in cavitation flow of a control valve. *International Journal of Heat and Mass Transfer*, 174, 121331. <https://doi.org/10.1016/j.ijheatmasstransfer.2021.121331>
12. Li, M., Yang, G., Wu, G., Li, X. (2020). Oxidative Deterioration Effect of Cavitation Heat Generation on Hydraulic Oil. *IEEE Access*, 8, 119720–119727. <https://doi.org/10.1109/access.2020.3005636>
13. Zhang, H., Chen, G., Wu, Q., Huang, B. (2022). Experimental investigation of unsteady attached cavitating flow induced pressure fluctuation. *Journal of Hydrodynamics*, 34 (1), 31–42. <https://doi.org/10.1007/s42241-022-0003-x>
14. Ferrari, A. (2017). Fluid dynamics of acoustic and hydrodynamic cavitation in hydraulic power systems. *Proceedings of the Royal Society A: Mathematical, Physical and Engineering Sciences*, 473 (2199), 20160345. <https://doi.org/10.1098/rspa.2016.0345>
15. Simpson, A., Ranade, V. V. (2018). Modeling hydrodynamic cavitation in venturi: influence of venturi configuration on inception and extent of cavitation. *AIChE Journal*, 65 (1), 421–433. <https://doi.org/10.1002/aic.16411>
16. Echouchene, F., Belmabrouk, H. (2022). Analysis of Geometric Parameters of the Nozzle Orifice on Cavitating Flow and Entropy Production in a Diesel Injector. *Applications of Computational Fluid Dynamics Simulation and Modeling*. <https://doi.org/10.5772/intechopen.99404>
17. Pilipenko, V. (1989). *Kavitatsionnye kolebaniya*. Kyiv: Naukova dumka, 316.
18. Oba, R., Ito, Y., Miyakura, H., Higuchi, J., Sato, K. (1987). Stochastic behavior (randomness) of acoustic pressure pulses in the near-subcavitating range. *JSME International Journal*, 30 (262), 581–586. <https://doi.org/10.1299/jsme1987.30.581>
19. Khozaei, M. H., Favrel, A., Miyagawa, K. (2022). On the generation mechanisms of low-frequency synchronous pressure pulsations in a simplified draft-tube cone. *International Journal of Heat and Fluid Flow*, 93, 108912. <https://doi.org/10.1016/j.ijheatfluidflow.2021.108912>
20. Tarasenko, T. V., Badach, V. M. (2019). Investigation of localization and intensity of calculative erosion in high-speed droselidation of liquid in hydrocontrol devices. *Problems of Friction and Wear*, 2 (83), 93–103. [https://doi.org/10.18372/0370-2197.2\(83\).13697](https://doi.org/10.18372/0370-2197.2(83).13697)
21. Khavari, M., Priyadarshi, A., Morton, J., Porfyakis, K., Pericleous, K., Eskin, D., Tzanakis, I. (2023). Cavitation-induced shock wave behaviour in different liquids. *Ultrasonics Sonochemistry*, 94, 106328. <https://doi.org/10.1016/j.ultsonch.2023.106328>
22. Melissaris, T., Schenke, S., van Terwisga, T. J. C. (2023). Cavitation erosion risk assessment for a marine propeller behind a Ro–Ro container vessel. *Physics of Fluids*, 35 (1). <https://doi.org/10.1063/5.0131914>
23. Joshi, S., Franc, J. P., Ghigliotti, G., Fivel, M. (2019). SPH modelling of a cavitation bubble collapse near an elasto-visco-plastic material. *Journal of the Mechanics and Physics of Solids*, 125, 420–439. <https://doi.org/10.1016/j.jmps.2018.12.016>
24. Magnotti, G. M., Battistoni, M., Saha, K., Som, S. (2020). Development and validation of the cavitation-induced erosion risk assessment tool. *Transportation Engineering*, 2, 100034. <https://doi.org/10.1016/j.treng.2020.100034>
25. Shi, H., Li, M., Nikrityuk, P., Liu, Q. (2019). Experimental and numerical study of cavitation flows in venturi tubes: From CFD to an empirical model. *Chemical Engineering Science*, 207, 672–687. <https://doi.org/10.1016/j.ces.2019.07.004>